

A PERFORMANCE ANALYSIS OF SOLAR CHIMNEY THERMAL POWER SYSTEMS

by

Mohammed Awwad Al-Dabbas

Mechanical Engineering Department, Mutah University, Karak, Jordan

Review paper

UDC: 66.011:697.329

DOI: 10.2298/TSCI101110017A

The objective of this study was to evaluate the solar chimney performance theoretically (techno-economic). A mathematical model was developed to estimate the following parameter: power output, pressure drop across the turbine, the max chimney height, airflow temperature, and the overall efficiency of solar chimney. The mathematical model was validated with experimental data from the prototype in Manzanares power

It can be concluded that the differential pressure of collector-chimney transition section in the system, is increase with the increase of solar radiation intensity.

The specific system costs are between 2000 €/kW and 5000 €/kW depending on the system size, system concept and storage size. Hence, a 50 MW_e solar thermal power plant will cost 100-250 M€. At very good sites, today's solar thermal power plants can generate electricity in the range of 0.15 €/kWh, and series production could soon bring down these costs below 0.10 €/kWh.

Key words: solar, wind, Jordan, max. height, solar chimney power plant, techno-economic

Introduction

Renewable are a source of green energy, environment friendly, but further important in the socioeconomic aspect, especially since they create thousands of green job opportunities, and can lead to a new regional industrial cluster.

Wind and solar alternatives are essential for growth, finance, and the political environment. The cost of wind power has reduced from the cost of power production from 9.5 cents per kilowatt-hour to 2 cents for wind energy production and to 7.7 cents for solar power production. This is very significant because developing countries, which depend on external sources to finance major energy projects, may be able to finance small scale solar and wind energies projects from their own resources and faster [1]. The objectives of this paper are: develop mathematical model to simulate study the performance of the solar chimney thermal power generating system [2], validate the result of the mathematical model with previously publish result (Manzanares prototype in Spain), analyze the potential for electric energy production in Mediterranean countries [3], estimate the quantity and price of the produced electric energy, and to determine the efficiency of the cycle, the power generated, the turbine

pressure drop, the overall efficiency of the solar chimney, and the cost of electric energy produced [4].

Solar characteristic in Jordan

Jordan relies, almost completely, on imported oil from neighboring countries, which causes a financial burden on the national economy [5]. Domestic energy resources, including oil and gas, cover only 3-4% of the country's energy needs. Jordan spends more than 7.5% of its national income on the purchase of energy. The levels of energy and electricity consumption will probably double in 15 years, and it is probable that annual primary energy demand will reach $8 \cdot 10^6$ ton of oil equivalent (toe) in 2010. Jordan accounts an average of $15.85 \cdot 10^3$ ton of emissions, of which CO_2 constitutes around 97%; fossil fuel combustion almost producing 85% by mass of the total GHG emissions [5].

Jordan is looking to harvest the wind and the Sun to lead the region in the use of renewable energy. The resource-poor country, which has no oil reserves and last year imported 96% of its fuel oil at a cost of 13% of its gross domestic product, has singled out renewable resources as key to its future development and security [6].

The drive for renewable resources is outlined in the Kingdom's national energy strategy, which calls for boosting solar and wind power's contribution to Jordan's energy mix from the current negligible level to 10% within 10 years, according to the Ministry of Energy and Mineral Resources [6].

Jordan has started its solar energy program 25 years ago in co-operation with many well-known scientific international institutions, and it is very popular nowadays [7]. As a result, Jordan is considered now as one of the leading countries in the region in the field of solar energy [7].

Jordan is blessed with an abundance of solar energy. Direct solar radiation in the Kingdom is estimated at 5.5 kWh/m^2 per day [6]. Winds in Aqaba and the Jordan valley have the potential of generating 145 GW/h per year enough to meet Jordan's needs and power a large portion of the Middle East region [6].

Jordan climate helped in expanding and developing solar energy use as an alternative to the ever expensive use of fuel. Around 40% of houses in Jordan installed solar heaters, in addition to hotels, clubs, hospitals, and schools. Solar systems can be worthy depending on the following factors: geographic location (temperature, sun shine, and wind speed), suitability of system for application, type of solar system, technology adapted in system manufacturing, quality of materials used in manufacturing, maintenance and post-sale services, and installation and operation [8].

Thus, Jordan is divided in five regions: the southern region ($29\text{-}30.5^\circ\text{N}$, $35\text{-}38^\circ\text{E}$); in this region, the annual daily average values of global irradiance are between 6 and 7 kWh/m^2 per day, the eastern region ($30.5\text{-}32.5^\circ\text{N}$, $36.5\text{-}39^\circ\text{E}$); in this region, the annual daily average values of global irradiance is about 5.0 kWh/m^2 per day, the middle region ($30.5\text{-}32^\circ\text{N}$, $35.5\text{-}36.5^\circ\text{E}$); in this region, the global irradiance is about 4.5 kWh/m^2 per day, the northern region ($32\text{-}33^\circ\text{N}$, $35.5\text{-}36.5^\circ\text{E}$); in this region the annual daily average value of global irradiance is about 5.5 kWh/m^2 per day, and the western region ($30.5\text{-}33^\circ\text{N}$, $35\text{-}35.5^\circ\text{E}$); in this region, the annual daily average values of global irradiance are between 4.5 and 5 kWh/m^2 per day. In general, the abundance of solar energy in Jordan is evident from the annual daily average of global solar irradiance, which ranges between 5 and 7 kWh/m^2 day on horizontal surfaces. This corresponds to a total annual value of $160\text{-}2300 \text{ kWh/m}^2$ per year [9].

Jordan is blessed with an abundance of solar energy, with high average daily solar radiation of 5 to 7 kWh/m², which is one of the highest in the world. The average sunshine duration is more than 300 days per year. National Energy Research Centre (NERC) is conducting a long term project for collecting and evaluating solar radiation to have new solar data. For this purpose, 14 measurement stations were installed around the country [10].

However, solar energy is not widely used, except for solar water-heaters, which are used for heating of domestic water. In addition to the economic benefit, the use of solar radiation instead of conventional fuels reduces the level of air pollutants; including greenhouse gas (GHG) emissions. In the year 2002, the total area of installed solar collectors in Jordan was more than 1,135,000 m² there are some other pilot applications in place. These include: solar desalination using solar heat pipe principle, solar desalination using solar still method, and parabolic trough desalination system in the city of Aqaba, photovoltaic brackish water reverse-osmosis desalination facility at Aqaba international industrial estate, and photovoltaic water pumping systems [10].

Solar chimney power plant

A technology of solar chimney power generation is not new in power generation sector, world over as shown in fig. 1 [11]. The Sun's radiation heats a large body of air, which is then forced by buoyancy forces to move as a hot wind through large turbines to generate electrical energy. Solar chimney power plants, with an output of 5-200 MW, require a transparent roof several kilometers in diameter, and the tube has to be as high as possible to achieve a large output. With the use of materials of better absorbing radiation, both the diameter of the base of the chimney as well as its height may be substantially reduced. On this basis, solar chimney plants are appropriate on land with no natural vegetation, such as desert regions [11].

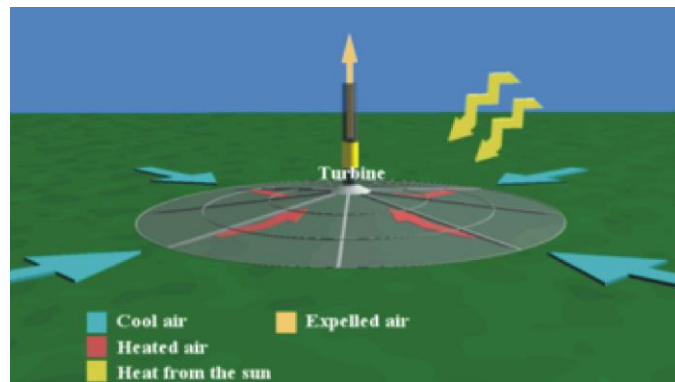


Figure 1. Solar chimney

Advantages of solar chimneys are:

- solar chimney power stations are particularly suitable for generating electricity in deserts and sun-rich wasteland,
- it provides electricity 24 hour a day from solar energy alone,
- no fuel is needed; it needs no cooling water and is suitable in extreme drying regions,
- it is particularly reliable and a little trouble-prone compared with other power plants,
- the materials concrete, glass and steel necessary for the building of solar chimney power stations are everywhere in sufficient quantities, and
- no ecological harm and no consumption of resources.

Disadvantages are:

- some estimates say that the cost of generating electricity from a solar chimney is five times higher than produced by gas turbine; although fuel is not required, solar chimneys have a very high capital cost, and
- the structure itself is massive and requires a lot of engineering expertise and materials to construct [2].

The characteristics of this solar chimney power plant are listed below [12].

- *Efficient solar radiation use.* The hot air collector used in the system, can absorb both direct and diffused radiation. Thus the solar chimney can operate on both clear and overcast days. The other major large-scale solar thermal power plants, which are often driven by high temperature steam generated from solar concentrators, can only use direct radiation.
- *Free dual functions, natural energy storage, and greenhouse effect.* The collector provides storage for natural energy, as the ground under the transparent cover can absorb some of the radiated energy during the day and releases it in the collector at night. Thus solar chimneys also produce a significant amount of electricity at night. The collector itself can also be used as a greenhouse, which will benefit agriculture production accordingly.
- *Low operation cost.* Unlike conventional power stations, and also other solar.
- *Thermal type power stations, solar chimneys do not need cooling water.* This is a key advantage in northwestern China where there have already been problems with drinking water.
- *Low construction cost.* The building materials needed for solar chimneys, mainly concrete and transparent materials are available everywhere in sufficient quantities. Particularly important is that no investment in a high-tech manufacturing plant is needed, as both wind turbine and solar collectors are well developed industrial products.

In its simplest form, the solar chimney consists of a black-painted chimney. During the day solar energy heats the chimney and the air within it, creating an updraft of air in the chimney. The suction created at the chimney's base can be used to ventilate and cool the building below.

There are however a number of solar chimney variations. The basic design elements of a solar chimney are:

- the solar collector area: this can be located in the top part of the chimney or can include the entire shaft; the orientation, type of glazing, insulation and thermal properties of this element are crucial for harnessing, retaining, and utilizing solar gains,
- main ventilation shaft: the location, height, cross-section and the thermal properties of this structure are also very important, and
- the inlet and outlet air apertures: the sizes, location as well as aerodynamic aspects of these elements are also significant.

A principle has been proposed for solar power generation, using a large greenhouse at the base rather than relying solely on heating the chimney itself.

Solar chimneys are painted black so that they absorb the Sun's heat more easily and efficiently. When the air inside the chimney is heated, it rises and pulls cold air out from under the ground via the heat exchange tubes [13].

The main cost of a solar updraft tower is in its construction. Operation and maintenance are minimal, with experiences at Manzanares suggesting that the cost of maintenance per installed capacity much lower than that of most other renewable, including wind geothermal, and conventional solar thermal plants.

In terms of operation and maintenance, solar updraft towers and solar panels are the easiest plants to run. Neither requires any consumable input. Both are very resistant to environmental exposure. Solar panels have no moving parts, and a broken unit can simply be wired out of a system. The one delicate part of a solar updraft tower, the turbine, is protected from the worst environmental effects at the base of the chimney. The rest of the plant also has very low failure rates.

Glass panels from the collector are relatively easily replaceable by local materials, and the plant can function acceptably with a low number of missing panels. Because of these infrequent failure and minimal input requirements, neither type of plant requires the attentions of a group of service personnel. While it is desirable to have a full time maintenance staff, these plants could be tended very infrequently.

The low maintenance requirements may also be an important factor in the decision to construct solar updraft towers in remote communities. Specialty replacement parts are not required for these plants; basic maintenance of the collector can be performed by those skilled in construction labor. The feathering turbine of a solar updraft tower is the only complex, actively controlled part in the system, but the turbine can function with the blades set at a fixed angle with a reduction in efficiency. In general, solar updraft towers are very robust.

Since the type of collector roof primarily determines a solar chimney's performance costs (the cleaning of the collector roof). A realistic collector roof for large-scale plants has to be built 2 to 6 meters above ground level. For this reason the lowest realistic height for a collector roof for large-scale technical use, 2 meters, was selected for the small Manzanares plant. (For output, a roof height of 50 cm only would in fact have been ideal.) Thus only 50 kW could be achieved in Manzanares, but this realistic roof height also permitted convenient access to the turbine at the base of the chimney. This also meant that experimental planting could be carried out under the roof to investigate additional use of the collector as a greenhouse.

On the other hand power towers share many of the same issues as trough plants; water use for evaporative cooling, maintenance costs for cleaning and operating the mirrors, and the inability to operate in cloudy conditions. Additionally, power towers have the disadvantage that they typically have to be built as large units, as opposed to many other solar technologies.

Solar thermal power plant concept – the solar chimney power plant – converts global irradiance in electricity. Since chimneys are often associated negatively with exhaust gases, this concept is also known as the solar power tower plant, although it is totally different from the tower concepts. A solar chimney power plant has a high chimney (tower), with a height of up to 1000 meters, and this is surrounded by a large collector roof, up to 130 meters in diameter, that consists of glass or resistive plastic supported on a framework (see artist's impression). Towards its centre, the roof curves upwards to join the chimney, creating a funnel [14].

The Sun heats up the ground and the air underneath the collector roof, and the heated air follows the upward incline of the roof until it reaches the chimney. There, it flows at high speed through the chimney and drives wind generators at its bottom. The ground under the collector roof behaves as a storage medium, and can even heat up the air for a significant time after sunset. The efficiency of the solar chimney power plant is below 2%, and depends mainly on the height of the tower, and so these power plants can only be constructed on land which is very cheap or free. Such areas are usually situated in desert regions. However, the whole power plant is not without other uses, as the outer area under the collector roof can also be utilized as a greenhouse for agricultural purposes. As with trough and tower plants, the

minimum economical size of solar chimney power plants is also in the multi-megawatt range [14].

Due to the poor part-load behavior of solar thermal power, plants should be installed in regions with a minimum of around 2000 full-load hours. This is the case in regions with a direct normal irradiance of more than 2000 kWh/m² or a global irradiance of more than 1800 kWh/m². These irradiance values can be found in the Earth's Sunbelt; however, thermal storage can increase the number of full-load hours significantly [14].

The potential for solar thermal power plants is enormous: for instance, about 1% of the area of the Sahara desert covered with solar thermal power plants would theoretically be sufficient to meet the entire global electricity demand. Therefore, solar thermal power systems will hopefully play an important role in the world's future electricity supply [14].

On other hand, the electricity production using solar energy is one of the main research areas at present in the field of renewable energies, the significant price fluctuations are seen for the fossil fuel, in one hand, and the trend toward privatization that dominates the power markets these days, in the other hand, will drive the demand for solar technologies in the near term [5].

The great importance of electricity from solar technologies is due to the considerable associated benefits (Schott, 2006, Haas, 2001, NEPCO, 2006, Badran, 2001, Alrobaei, 2008), namely: maximum power generation at peak load hours in hot climate countries, the modular character, the off grid solar power production for remote locations, reduction of GHG emissions, increases in local employment and income, enhanced local tax revenues, more diversified resource base, security of power supplies, economic flexibility due to modular, dispersed, and smaller scale technologies, reduction or elimination of pollution associated with electricity production, contribution towards sustainability, and other benefits beside power generation *i. e.*, fresh water [5].

Solar power has the advantage of electricity generation at peak load hours. Hot climate countries, like Jordan, have the highest electricity peak load consumption in demands during the hot summer days [5].

Solar power plants play an important role in decreasing the environmental pollution; they contribute directly to the CO₂ reduction that caused by the conventional fossil fuel power plants. According to the Greenpeace study, the use of solar power plants can avoid 362 million tons of CO₂ emissions worldwide from 2002 to 2025 (Brakmann *et al.*, 2005) [5].

Literature review

The solar chimney power plant system, which consists of four major components, collector, chimney, turbine, and energy storage layer, was first proposed in the late 1970s by Professor Jörg Schlaich and tested with a prototype model in Manzanares, Spain, in the early 1980s. In the recent years, more and more researchers have shown strong interest in studying such solar thermal power generating technology for its huge potential of application all over the world. Four pilot solar chimney power models were in succession built by Krisst, Kulunk, Pasurmarthi and Sherif, and Zhou *et al.* The researchers also carried out experimental investigations on the performances of the models. More theoretical investigation and simulations have been carried out by Padki and Sherif, Lodhi, Bernardes *et al.*, von Backström and Gannon, Gannon and von Backström, Pasthan *et al.*, Schlaich *et al.*, Bilgen and Rheault, Pretorius and Kröger, Ninic, Onyango and Ochieng [15].

Haaf *et al.* provided fundamental studies for the Spanish prototype in which the energy balance, design criteria and cost analysis were discussed and reported preliminary test results of the solar chimney power plant [36]. Bernardes *et al.* developed a comprehensive thermal and technical analysis to estimate the power output and examine the effect of various ambient conditions and structural dimensions on the power output [37]. Pasthor *et al.* carried out a numerical simulation to improve the description of the operation mode and efficiency by coupling all parts of the solar chimney power plant including the ground, collector, chimney, and turbine [38]. Schlaich *et al.* presented theory, practical experience, and economy of solar chimney power plant to give a guide for the design of 200MW commercial solar chimney power plant systems [39]. Ming *et al.* presented a thermodynamic analysis of the solar chimney power plant and advanced energy utilization degree to analyze the performance of the system, which can produce electricity day and night [40]. Liu *et al.* carried out a numerical simulation for the MW-graded solar chimney power plant, presenting the influences of pressure drop across the turbine on the draft and the power output of the system [41]. Bilgen and Rheault designed a solar chimney system for power production at high latitudes and evaluated its performance [42]. Pretorius and Kröger evaluated the influence of a developed convective heat transfer equation, more accurate turbine inlet loss coefficient, quality collector roof glass, and various types of soil on the performance of a large scale solar chimney power plant [43].

Ming *et al.* presented a mathematical model to evaluate the relative static pressure and driving force of the solar chimney power plant system and verified the model with numerical simulations. Later, they developed a comprehensive model to evaluate the performance of a solar chimney power plant system, in which the effects of various parameters on the relative static pressure, driving force, and efficiency have been further investigated [44, 45]. Zhou presented experiment and simulation results of a solar chimney thermal power generating equipment in China, and based on the simulation and the specific construction costs at a specific site, the optimum combination of chimney and collector dimensions was selected for the required electric power output [46]. (See also [36-46].)

Numerical solution

It is unpractical to establish a solar chimney power plant system (SCPPS) used to experimental research for being a large scale system. Using the Spanish prototype plant as simulation object, the SCPPS is numerical simulation calculated [16]. It might be a little difficult to carry out the numerical simulations on the solar chimney power plant systems coupled with the collector, chimney and turbine [15]. The main factors that influence on the performance of the SCPPS have been simulated. The effects on the flow field of the SCPPS which caused by solar radiation intensity have been analyzed. The calculated results are approximately equivalent to the relative experimental data of the prototype. It shows the dependability of the simulative results and the validity of the simulation methods [16].

Generally, there are three methods to obtain solution in exact study on characteristic solar chimney power plant [17]:

- (1) The analytical method, expected to produce solution of differential equations in analytical form (successful in very simplified case). From solving of differential problem the ordinary solvable equations can be obtained. Usually introduction of many simplifying assumptions allows for passing over the stage of formulation of differential equations and directly developing regular algebraic equations which can be solved if the number of un-

knowns is not larger than the number of derived equations. The present study belongs to this category.

- (2) Numerical method, solving numerically by developing differential equations into the finite difference equations, which allow for significantly less simplifying assumptions. However, the numerical method, replacing the analytical approach, itself brings some inadequacy by variables presented discretely.
- (3) Method based on similarity theory. According to this theory the characteristic dimensionless simplexes (similarity criteria) are extracted from differential equations. The criteria are used for derivation of mutual relations based on experimental data from the appropriately programmed measurements. The relations are fragmentary particular solutions, and have a meaning of particular integral of differential problem. In order to formulate an interpretative model of a process the similarity theory may apply experimental data obtained on laboratory, pilot or commercial scale. The method has not been applied yet to a SCPP.

The main assumptions used in numerical models and simulation in this paper are [17]:

- the floor is perfectly black; the deck material is perfectly transparent for solar radiation ($\tau_d = 0.95$, $\alpha = 1$),
- the chimney material is perfectly black,
- air is perfectly transparent for radiation,
- air is considered as an ideal gas *i. e.* $p = \rho RT$, and
- the relative air pressure drop during the expansion in the turbine $r_t = (\rho_1 - \rho_2)/(\rho_1 - \rho_3) = 2/3$ was used (this is the same assumption of Von Backström *et al.* [18]).

It should be mentioned that many authors were assumed different values of relative air pressure drop r_t during expansion in the turbine. The relative air pressure drop was assigned 0.66 by Mullet (1987), 0.97 by Bernardes *et al.* (2003), 0.66 by Von Backström *et al.* On other hand, Backström, Fluri, and later Nizetic concluded that the real value of the relative air pressure drop lies between the 0.8-0.9. Our assumption of the optimum ratio was based on the analytical validation did by Von Backström *et al.* [18].

The basic governing differential equations that describe the flow inside the solar chimney are:

– continuity equation [19, 20]

$$\frac{\partial \rho}{\partial t} + \frac{\partial(\rho u)}{\partial x} + \frac{\partial(\rho v)}{\partial y} + \frac{\partial(\rho w)}{\partial z} = 0$$

– momentum equations [18-20]

$$\frac{\partial(\rho u)}{\partial t} + \frac{\partial(\rho uu)}{\partial x} + \frac{\partial(\rho vu)}{\partial y} + \frac{\partial(\rho wu)}{\partial z} = -\frac{\partial p}{\partial x} + \mu \left(\frac{\partial^2 u}{\partial x^2} + \frac{\partial^2 u}{\partial y^2} + \frac{\partial^2 u}{\partial z^2} \right)$$

$$\frac{\partial(\rho v)}{\partial t} + \frac{\partial(\rho vu)}{\partial x} + \frac{\partial(\rho vv)}{\partial y} + \frac{\partial(\rho wv)}{\partial z} = -\frac{\partial p}{\partial y} + \mu \left(\frac{\partial^2 v}{\partial x^2} + \frac{\partial^2 v}{\partial y^2} + \frac{\partial^2 v}{\partial z^2} \right)$$

$$\frac{\partial(\rho w)}{\partial t} + \frac{\partial(\rho wu)}{\partial x} + \frac{\partial(\rho wv)}{\partial y} + \frac{\partial(\rho ww)}{\partial z} = \rho g \beta (T - T_\infty) + \mu \left(\frac{\partial^2 w}{\partial x^2} + \frac{\partial^2 w}{\partial y^2} + \frac{\partial^2 w}{\partial z^2} \right)$$

– energy equation [21]

$$\frac{\partial(\rho cT)}{\partial t} + \frac{\partial(\rho cuT)}{\partial t} + \frac{\partial(\rho vcT)}{\partial y} + \frac{\partial(\rho wcT)}{\partial z} = \lambda \left(\frac{\partial^2 v}{\partial x^2} + \frac{\partial^2 v}{\partial y^2} + \frac{\partial^2 v}{\partial z^2} \right)$$

– k-ε model [19-23]

$$\begin{aligned} \frac{\partial}{\partial T}(\rho k) + \frac{\partial}{\partial x_i}(\rho k u_i) &= \frac{\partial}{\partial x_i} \left[\left(u + \frac{u_t}{\sigma_k} \right) \frac{\partial k}{\partial x_i} \right] + G_X + G_b + \rho \varepsilon + S_k \\ \frac{\partial(\rho \varepsilon)}{\partial t} + \frac{\partial}{\partial x_i}(\rho \varepsilon u_i) &= \frac{\partial}{\partial x_i} \left[\left(u + \frac{u_t}{\sigma_\varepsilon} \right) \frac{\partial \varepsilon}{\partial x_i} \right] + c_{1\varepsilon}(G_k + C_{3\varepsilon} + G_b) - c_{2\varepsilon} \rho \frac{\varepsilon^2}{k} + s_3 \\ c_{1\varepsilon} &= 1.44; \quad c_{2\varepsilon} = 1.92; \quad c_\mu = 0.09; \quad \sigma_k = 1.0; \quad \sigma_\varepsilon = 1.3 \end{aligned} \quad [23]$$

where G_k is the generation of turbulence kinetic energy due to mean velocity gradients, and G_b – the generation of turbulence kinetic energy due to buoyancy [23].

The whole system should be divided into three regions: the collector, the turbine, and the chimney [24, 25]. The Rayleigh number of the SCPPS is higher than the critical Rayleigh number, 109, which means that turbulent flow happens almost in the whole system [16].

The pressure difference which is produced between the chimney base and the ambient is presented by [26]:

$$\Delta p = g \int_0^H [\rho_\infty(h) - \rho(h)] dh = \Delta p_t + \Delta p_f + \Delta p_{in} + \Delta p_{out}$$

where $\Delta p_f = f(H/p)(1/2)(\rho V^2)$ is the friction loss, $\Delta p_{in} = \varepsilon_{in}(1/2)(\rho_{in} v_{in}^2)$ – the entrance loss, $\Delta p_{out} = \varepsilon_{out}(1/2)\rho_{out} V_{out}^2$ – the exit kinetic energy loss, and Δp_t is kinetic energy transferred to the turbine. The following coefficients are used: $f = 0.008428$, $\varepsilon_{in} = 0.056$, and $\varepsilon_{out} = 1.058$

Consequently:

$$\Delta p = 0.00353gH \left[\frac{\pi G \eta_{coll}}{C_p \dot{m}} R_{coll}^2 - \frac{g}{2C_p} H + \frac{1}{2} \gamma_\infty H \right]$$

where the mass flow of hot air passing through the chimney (\dot{m}) is:

$$\dot{m} = \rho_{in} V_{in} A_C$$

The electric power generated by the turbine generators, P_{out} , can be expressed as [27]:

$$P_{out} = \eta_{tg} \Delta p_t V A_C$$

where η_{tg} is the efficiency of turbine generators [28]. Total energy conversion efficiency can be expressed as the ratio of P_{out} to solar radiation input on the collector [29]:

$$\eta = \frac{P_{out}}{\pi R_{out}^2 G}$$

The maximum chimney height H_{max} is:

$$H_{max} = \frac{C_p \dot{m}}{U \pi D} \ln \left[\frac{\pi^2 U D G \eta_{coll} R_{coll}^2}{C_p \dot{m}^2 (g - \gamma_\infty C_p)} + 1 \right]$$

where $m = \rho_{in} v_{in} A_C$.

Description and validation of the small-scale chimney power plant in Spain

In 1982, a small-scale experimental model of a solar chimney power plant was built under the direction of German engineer J. Schlaich in Manzanares, Ciudad Real, 150 km south of Madrid, Spain; the project was funded by the German government [29].

The chimney had a height of 195 metres and a diameter of 10 metres with a collection area (greenhouse) of 46.000 m² or 244 m diameter obtaining a maximum power output of about 50 kW. However, this was an experimental set-up that was not intended for power generation. Instead, different materials were used for testing such as single or double glazing or plastic (which turned out not to be durable enough), and one section was used as an actual greenhouse, growing plants under the glass. During its operation, optimization data was collected on a second-by-second basis with 180 sensors measuring inside and outside temperature, humidity and wind speed. For the choice of materials, it was taken into consideration that such an inefficient but cheap plant would be ideal for third world countries with lots of space – the method is inefficient for land use but very efficient economically because of the low operating cost. So cheap materials were used on purpose to see how they would perform, such as a chimney built with iron plating only 1.25 mm thick and held up with guy ropes. For a commercial plant, a reinforced concrete tower would be a better choice. This pilot power plant operated for approximately eight years but the chimney guy rods were not protected against corrosion and not expected to last longer than the intended test period of three years. So, not surprisingly, after eight years they had rusted through and broke in a storm, causing the tower to fall over. The plant was decommissioned in 1989. Based on the test results, it was estimated that a 100 MW plant would require a 1000 m tower and a greenhouse of 20 km². Because the costs lie mainly in construction and not in operation (free fuel, little maintenance and only 7 personnel), the cost per energy is largely determined by interest rates and years of operation, varying from 5 c€ per kWh for 4% and 20 years to 15 c€ per kWh for 12% and 40 years [30].

To validate the simulation results presented by the author in this paper, numerical simulation results are compared with: the experimental result for the Spanish prototype solar chimney [17, 31] and CFD modeling.

Computational fluid dynamics modelling of the turbine [3, 33]

As real experiments in this type of flow are very expensive and time consuming, at this early stage it should be sufficient to perform “numerical experiments” to verify the validity of the proposed similarity because computational fluid dynamics (CFD) has over time proven to be quite a reliable tool in fluid dynamic research and application especially when only global phenomena is being sought after. CFX was chosen since it has been widely accepted in the research and application communities and partly because of its versatility with grid generation and boundary conditions. For this purpose, CFX solves the conservation equations for mass, momentum, and energy using a finite volume method. Adaptive unstructured tetrahedral meshes are used in the present study. The plants studied are modeled as axis-symmetry where the centerline of the chimney is the axis of symmetry.

Mathematical turbine models numerous analytical investigations to predict the flow in solar chimney had been proposed (Gannon *et al.*, 2000; Haaf *et al.*, 1983; Padki *et al.*,

1988; Padki *et al.*, 1989a; Padki *et al.*, 1989b; Padki *et al.*, 1992; Schlaich, 1995; Von Backström *et al.*, 2000; Yan *et al.*, 1991).

There are common features of all these investigations in that they developed mathematical models from the fundamental equations in fluid mechanics. In doing this the temperature rise due to solar heat gain had been assumed to be a reasonable value using engineering intuition. Flows in the roof and the chimney were studied individually without a mechanism to let them interact.

Chitsomboon (2001a) proposed an analytical model with a built-in mechanism through which flows in various parts of a solar chimney can naturally interact. Moreover, thermo mechanical coupling was naturally represented without having to assume an arbitrary temperature rise in the system.

When the turbine modeling is performed the following parameter have to be defined:

- geometry definition; the geometry of the flow passage and the turbine is defined; it is assumed that the diameter of the chimney is given and hence the chimney inlet area is known; the number of turbines is specified; the blade aspect ratio, and the hub-to-tip radius ratio is set; choose operating conditions; the operating point and the working fluid are specified; the operating point is given with inlet total temperature, inlet total pressure, and exit total pressure,
- the working fluid is assumed to be dry air,
- set bounds for optimization,
- choose speed for rotor,
- initial guess; an initial guess for the total-to-total turbine efficiency and the design variables,
- evaluation of initial parameters; the axial components of the chimney inlet and the turbine exit flow velocities are optimize for total-to-static efficiency; utilizing the specific turbine model, which will be described in detail below, an optimization algorithm is run to get the maximum total-to-static efficiency at this particular speed of the first rotor; as long as the total-to-total efficiency value has not converged,
- we iterate at each iteration, the efficiency result is taken as the new initial guess, and
- detect optimal speed of rotor; new iterations are executed with new values for the speed of rotor until the speed providing the maximum total-to-static efficiency has been detected.

Over the last decades CFD has evolved immensely and today many Navier-Stokes solvers are available. Some of them are capable of solving unsteady 3-D multistage turbine flow with leakage and cavity flow included. The primary gas path flow in particular is predicted reasonably well. There are, however, still many areas of ongoing research, for example the modeling of turbulence, transition, and secondary flow.

In the design and analysis of gas turbines CFD is used extensively and many publications can be found; *e. g.* Rosic *et al.* (2006) point out the importance of shroud leakage modelling in turbine flow computations. Praisner and Clark (2007) and Praisner *et al.* (2007) discuss the prediction of transition. Pullan (2006) looks at secondary flows and loss caused by blade row interaction in a turbine stage. Also in other turbine applications CFD becomes increasingly important; *e. g.* Thakker *et al.* (2005) use CFD to analyze an impulse turbine for wave energy power conversion and Sezer-Uzol *et al.* (2006) present a time-accurate three dimensional simulation of the flow field around a horizontal axis wind turbine rotor.

The scope of the investigation is to do a first evaluation of a commercial CFD package as a tool in context with solar chimney turbines. 3-D simulations of both the single vertical axis and the multiple horizontal axis turbine models are presented, and the results are compared to experimental data. Structured grids are used by this package and preconditioning and multi grid acceleration are implemented. This software package has been chosen mainly for its excellent turbo machinery grid generation capabilities, which made it possible to generate high quality grids even for the rotor row, where the blades are highly twisted.

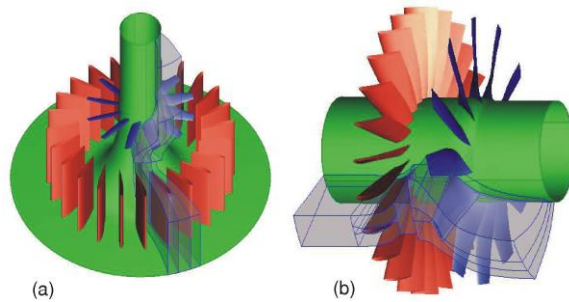


Figure 2. Computational domains for the single turbine model (a) and the multiple turbine model (b)

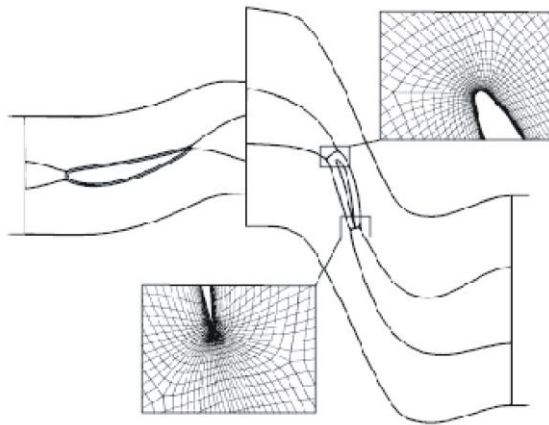


Figure 3. Schematic of mesh block boundaries and a typical computational mesh around the rotor leading and trailing edge at the tip of the multiple horizontal axis turbine model geometry

the computational domain, *i. e.* a straight shroud is assumed down stream of the turbine in both cases.

Convergence. With the finest multi grid level convergence is usually achieved after 200 iterations; residuals have diminished by more than 5 orders of magnitude, the mass flow error is smaller than 0.1% and the torque, axial thrust and efficiency values have also converged. The convergence criterion was set to 10^{-4} for the continuity, to 10^{-5} momentum and turbulence equations while for energy the criterion was 10^{-8} and for radiation 10^{-7} .

The computational grids. The computational domains for two turbines are shown in fig. 2. Figure 3 shows the block boundaries at the shroud of the multiple horizontal axis turbine model geometry. A skin topology was chosen for both blade rows, *i. e.* each blade is surrounded by an O-mesh block, the skin block, and four H-mesh blocks, which connect the skin block to the periodic boundaries as well as the inlet and outlet boundaries of the blade row. Additional H-blocks extend the flow domain to the upstream and downstream boundaries.

The meshes around the trailing and the leading edge of the rotor blade are shown in fig. 4. In the rotor blade rows fully non-matching periodic boundaries were used. This makes meshing much easier, particularly for blades with high stagger angles. Shroud leakage flow was not modelled. The grid for the single vertical axis model turbine was setup in a similar fashion

While the hubs of both model turbines end immediately downstream of the rotor trailing edges, for the simulation the hubs are extended to the outlet boundary. The diffuser after the single turbine is not represented in

Boundary conditions. Proper boundary conditions are needed for a successful computational work. At the roof inlet, the total pressure and temperature are specified; whereas at the chimney exit the “outlet” condition with zero static pressure is prescribed. Additionally, the “symmetry” boundary conditions are applied at the two sides of the sector. The adiabatic free slip conditions are prescribed to the remaining boundaries [3, 33].

As specified above that frictionless flow be modeled, then the free-slip conditions are applied to all walls. All test cases were computed until residuals of all equations had reached their respective minimum. Moreover, global conservation of mass had been re-checked to further ascertain the convergence of the test cases. For the multiple turbine models the boundary conditions are summarized in tab. 1.

Post processing. The CFD results were evaluated with CFView, which is the flow visualization tool for FINE/Turbo. The grid lines used for the profile data extraction are indicated in figs. 3 and 4.

Figures 5 and 6 shows the average velocity along the flow path; it can be seen that the velocities of the flow under the roof increase along the flow path and remains constant along the tower. The temperature profiles, shown in fig. 7, also demonstrate similar behaviors as the velocity profiles.

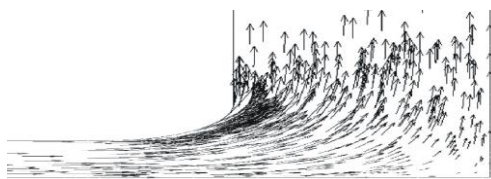


Figure 5. Typical velocity field around the junction of the roof and the chimney [32a]

In fig. 8, the pressure distributions are seen to be nominally constant under the roof before falling linearly in the tower portion, to meet the hydrostatic pressure distribution at the tower top. Note that the ordinate is the gauge pressure scaled such that pressures at the top of tower are always zero.

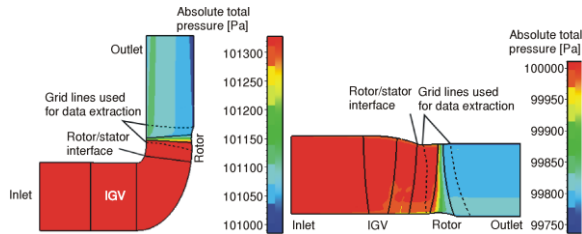


Figure 4. Meridional view of flow domains of the multiple turbine (left) and the single turbine geometry, showing a contour plot of absolute total pressure and indicating the grid lines used for the profile data extraction (color image see on our web site)

Table 1. List of boundary conditions for the CFD analysis of the multiple turbine models

| | |
|----------------------------|--------------------------|
| Inlet total temperature | 300 K |
| Inlet total pressure | 100 000 Pa |
| Exit static pressure | 99 720 Pa |
| Inlet flow angle | ± 0 |
| Inlet turbulence viscosity | 0.0001 m ² /s |
| Blade speed at mean radius | 33.74 m/s |

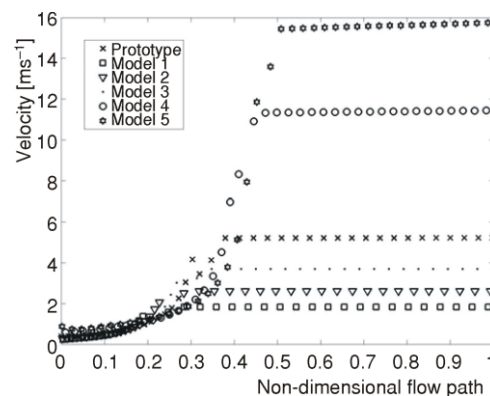


Figure 6. Numerical prediction of velocity profiles for insolation of 800 W/m²

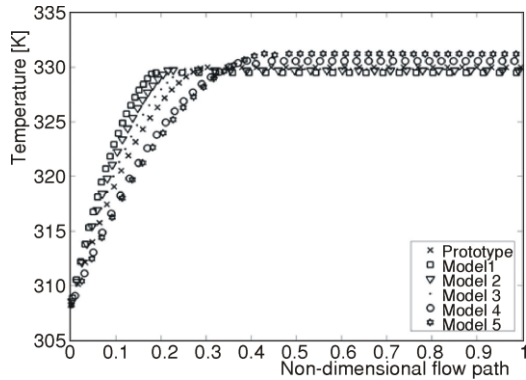


Figure 7. Numerical prediction of temperature profiles for insolation of 800 W/m^2

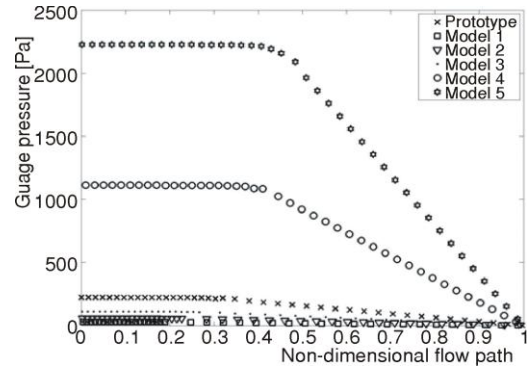


Figure 8. Numerical prediction of pressure profiles for insolation of 800 W/m^2

Simplified model for calculation of the solar chimney power plant performances

A computer program was written to compute the result of the simulation model to evaluate the performance of solar chimney.

Also, in this section our simulated results of the proposed simplified model was presented and compared with the previous experimental readings from the prototype in Manzanares. The comparisons were performed to verify the proposed simplified model is satisfied for evaluation the performance of solar chimney.

In general, there are in relatively good agreement between the results of the simulations and the results of the experimental readings from Spanish prototype [34].

Mutah University pilot solar chimney

Figure 9 show the first pilot solar chimney which was built in Mutah, Jordan (for more details see Appendix).

Figures 10 and 11 show the effect of the ambient temperature and the solar irradiance on chimney power productivity. The solar radiation, however, is in a dominant position to affect the power generation in the solar chimney, in comparison to the ambient temperature.



Figure 9. The first pilot solar chimney on Mutah, Jordan

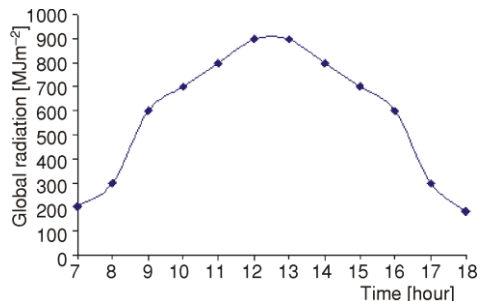


Figure 10. Global radiation in Mutah University (May 2009)

Many factors affect on power generation and may influence the performance of the solar chimney plant such as: the materials used to make the solar chimney, solar chimney height, solar collector materials, and the soil or rock contents under the solar collector and wind speed [12].

The chimney efficiency, η_{sc} is expressed as:

$$\eta_{sc} = \frac{P_{tot}}{Q} = \frac{gH_{sc}}{C_p T_o}$$

where, H_{sc} is the height of the chimney,

The power contained in the flow, P_{tot} , is:

$$P_{tot} = \frac{gH_{sc}}{T_o} \rho_{coll} V_c \Delta T A_c$$

The pressure difference, Δp_{tot} , which is produced between the chimney base and the surroundings is:

$$\Delta p_{tot} = \rho_{coll} g H_{sc} \frac{\Delta T}{T_o}$$

The maximum mechanical power taken up by the turbine is:

$$P_{wt,max.} = \frac{2}{3} V_c A_c \Delta p_{tot}$$

Thus the produced electrical power from the solar chimney to the grid is:

$$P_e = \frac{2}{3} \eta_{coll} \eta_{wt} \frac{g}{C_p T_o} H_{sc} A_{coll} G$$

Figures 12 and 13 show the power output from the solar chimney to the grid vs. solar time, and rotational speed using the derived produced electrical power equation. As shown in figs. 10 and 11 the variations in solar irradiance and power production behave similarly. The better the solar radiation, the higher the capacity of power production will be

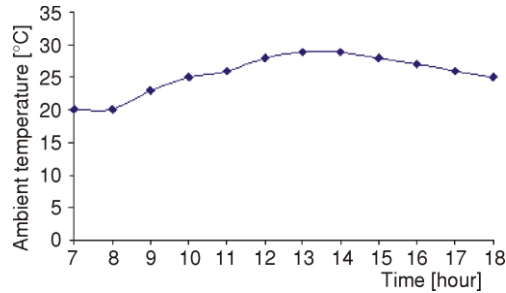


Figure 11 Ambient temperature in Mutah University (May 2009)

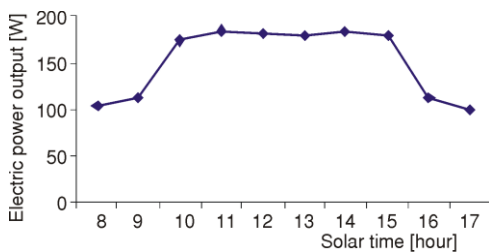


Figure 12. The computed electric power output vs. solar time in Mutah University

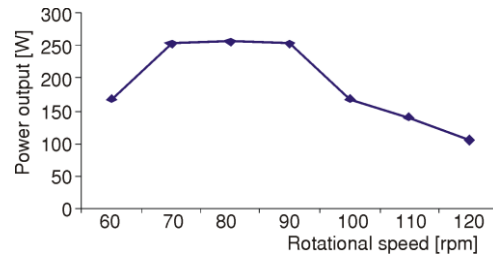


Figure 13. The computed power output vs. rotational speed in Mutah University

the power generation may be further increased if the chimney efficiency, which increases with the increase of chimney height, could be improved.

Figures 14 and 15 show the power output vs. solar time and rotational speed from a prototype solar chimney power plant in Manzanares, Spain. In general good agreement were obtained between simulated result and previous publish measured data.

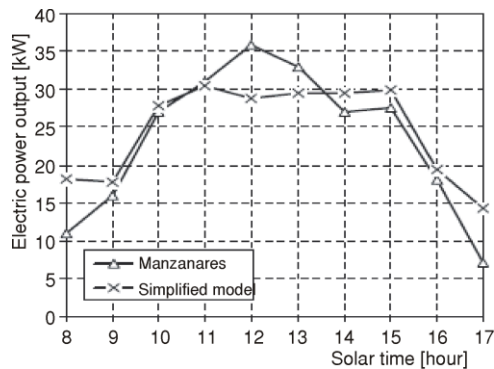


Figure 14. The experimental results from a prototype solar chimney power plant in Manzanares, Spain [3]

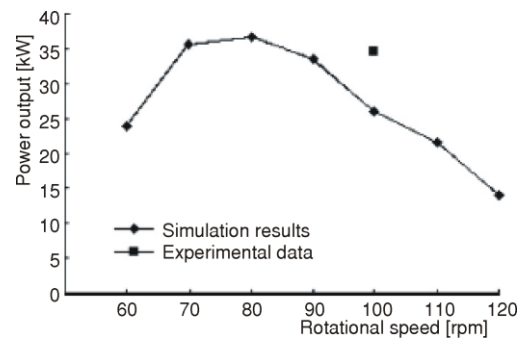


Figure 15. Power output vs. rotational speed from a prototype solar chimney power plant in Manzanares, Spain [3]

The maximum chimney height was calculated using empirical relation equation. Figure 16 shows the computed H_{\max} from the simulated model.

Figure 17 shows the actual measured values of H_{\max} based on the Manzanares prototype solar chimney power plant. As shown in fig. 17. An agreement between all actual H_{\max} and simulated result within a maximum difference of 1.14% were obtained.

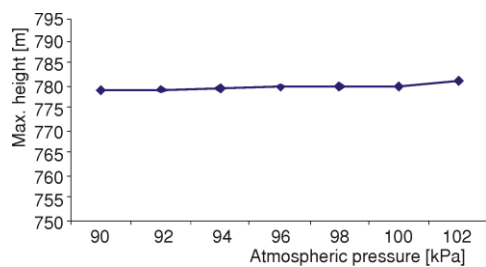


Figure 16. Maximum computed chimney height from a prototype solar chimney power plant

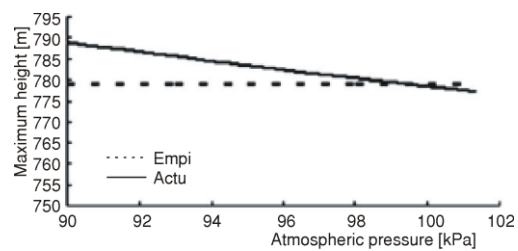


Figure 17. Maximum chimney height from a prototype solar chimney power plant in Manzanares, Spain [3]

A very important factor for optimal electrical power output is the pressure drop at the turbine, which corresponds to the maximum electric power output for a given condition.

Figure 18 shows the computed pressure drop at the turbine from simulated model.

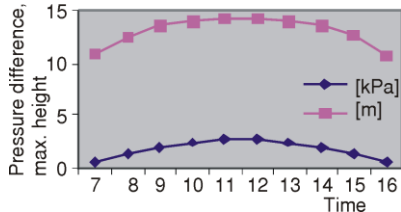


Figure 18. Computed pressure drop of the turbine and mass flow rate

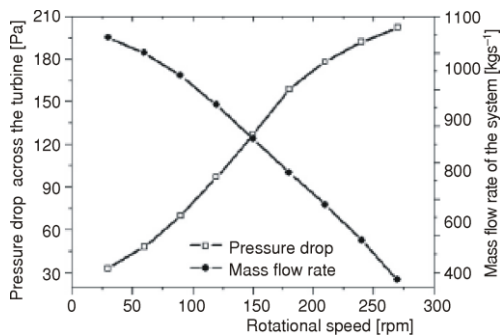


Figure 19. Pressure drop of the turbine and mass flow rate from a prototype solar chimney power plant in Manzanares, Spain [3]

solar chimney power plant. In general an agreement for air flow temperature rise was obtained.

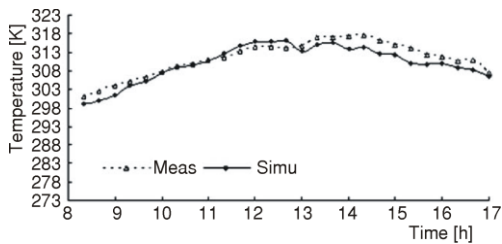


Figure 21. Airflow temperature in chimney during the day from a prototype solar chimney power plant in Manzanares, Spain [3]

Figure 19 shows the actual measured values of the pressure drop at the turbine based on the Manzanares prototype solar chimney power plant.

Figure 20 show the computed air flow temperature rise in the solar chimney during the day from:

$$T(h) = T_{\infty, \text{in}} - \frac{gh}{C_p} + \frac{\pi \eta_{\text{coll}} G^2}{C_p m^{\circ}} R_{\text{coll}}^2$$

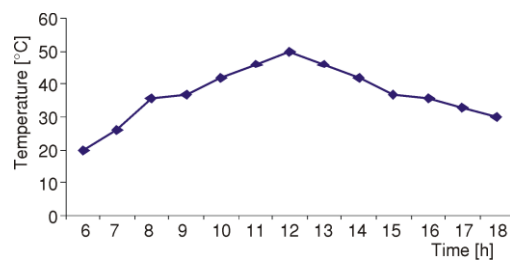


Figure 20. The computed airflow temperature in chimney during the day [3]

Figures 21 and 22 show the measured temperature rise in the solar chimney during the day based on the Manzanares prototype

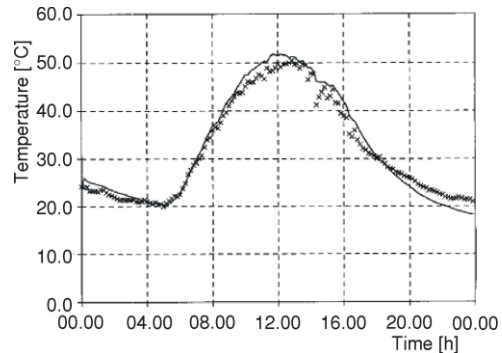


Figure 22. Airflow temperature in collector during the day from a prototype solar chimney power plant in Manzanares, Spain [3]

The overall efficiency of solar chimney power plant is:

$$\eta_{\text{sp}} = \frac{\dot{m} C_p \Delta T}{A_{\text{coll}} G} \frac{g H_c}{C_p T_o} \left(1 - \frac{w_c^2}{2 C_p \Delta T \eta_{\text{sc}}} \right) \eta_{\text{sc}}$$

Figure 23 shows the overall efficiency of solar chimney power plant as a function of air flow velocity at the chimney inlet which computed from previous equation.

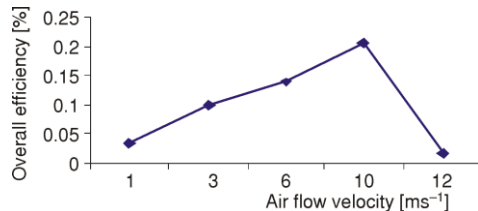


Figure 23. Overall efficiency of solar chimney vs. air flow velocity

Economic aspects of electric energy production

A solar updraft power station would require a large initial capital outlay, but would have relatively low operating cost. However, the capital outlay required is roughly the same as next-generation nuclear plants such as the AP-1000 at roughly 5 \$/W of capacity. Like other renewable power sources there would be no cost for fuel. A disadvantage of a solar updraft tower is the much lower conversion efficiency than concentrating solar power stations have, thus requiring a larger collector area and leading to higher cost of construction and maintenance [30].

The solar tower plant capital investment includes the chimney, collector roof, and turbine assembly construction costs. The cost structure, relative to the overall investment, is as follows [3]:

- the chimney bears approximately 30-50% of costs,
- the collector roof constitutes about 20-40% of the expenditures,
- testing and commissioning amount to 6-10% of the total investment, and
- annual operation and maintenance costs amount to 4-5% of the total investment.

Depending on the nominal plant power medium, the orientation price for a collector roof made of single glass amounts to 6.0-9.0 €/m², while that of the chimney, which is made of reinforced concrete, amounts to 250-500 €/m². It is important to say that reinforced concrete chimney is more expensive than a chimney made of steel. The turbine assembly cost analyses are more complex. The portion in the total cost of solar chimney plant incurred by the turbine increases with decreasing of nominal power of the turbine. For a nominal power of 200 MW, for example, the overall specific turbine expenses amount to 700 €/kW_e, while, for a power of 5 MW, they amount to 1600 €/kW_e. The above-mentioned costs for the individual components of the solar power plant are intended for reference purposes only and depend on the nominal power of the plant and the performance of the specifically designed collector roof. The costs indicated above include labor costs [3].

Consequently, the overall cost of solar chimney plant included the following requirement investment [3]:

- collector roof: approximately 10.0 M€,
- chimney: approximately 35.0 M€,
- Turbines: approximately 8.0 M€, and
- engineering, tests, misc.: approximately 7.0 M€.

Total invested capital: $K_o = 60.0$ M€

The average costs of produced electrical energy are calculated from:

$$k_w = \frac{K_o}{E_{el,an} n} \sum_{t=1}^n \left(\frac{f_w}{(1+r_{in})^t} + r_b \right)$$

$$P_e = \frac{A_{coll}}{G \eta_{coll} \eta_{sc} \eta_t \eta_{wt}}$$

where, $E_{e,an}$ [MWh per year] is the average annual electric energy produced; and it would range from 5.0 to 6.0 GWh per year, n – the amortization period and its equal 20-40 years, r_b – the maintenance and repair costs equal 5.5% per year, and r_t – the rate of inflation = 6.0% per year. Factor f_w is the defined as:

$$f_w = \frac{(1+p)^n p}{(1+p)^n - 1}$$

where p is the calculated interest rate.

The results of the calculations for the two locations, depending upon the calculated interest rate and period of amortization, are shown in fig. 24 [3].

As shown in fig. 24, we conclude that the average price of electrical energy kWh produced by a solar chimney power plant in the Mediterranean region would range between 0.24 and 0.78 €/kWh.

There is still a great amount of uncertainty and debate on what the cost of production for electricity would be for a solar updraft tower and whether a tower (large or small) can be made profitable. Schlaich *et al.* [39] estimate a cost of electricity between 7 (for a 200 MW plant) and 21 (for a 5 MW plant) c€ per kWh, but other estimates indicate that the electricity cannot possibly be cheaper than 25-35 c€ per kWh. Compare this to LECs of approximately 3 c€ per kWh for a 100 MW wind or natural gas plant. No reliable electricity cost figures will exist until such time as actual data are available on a utility scale power plant, since cost predictions for a time scale of 25 years or more are unreliable [31].

Figure 25 show the energy production costs from solar chimneys, compared to coal and combined cycle power plants depending on the interest rate and based on equal and common methods [35].

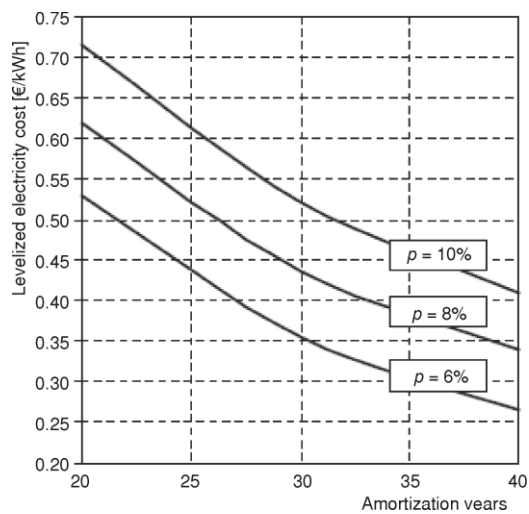


Figure 24. Influence of amortization period on leveled electricity cost

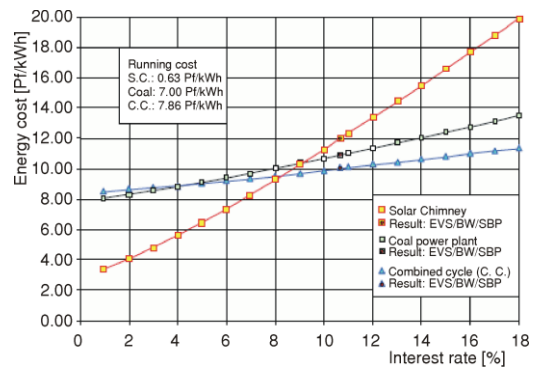


Figure 25. Energy production costs from solar chimneys, coal, and combined cycle power plants depending on the interest rate

Conclusions

A numerical simulation method for the solar chimney power plant system was done. The results of comparison between the simulated model and the Spanish prototype with a 3-blade turbine show that with the increase in the turbine rotational speed, the average velocity of the chimney outlet and the system mass flow rate decrease, the average temperature of the chimney outlet and the turbine pressure drop inversely, while the maximum available energy, power output, and efficiency of the turbine each has a peak value.

Also, the power generation capacity increases with the increase in solar chimney height and solar collector area. It is also found that the higher the solar irradiance, the higher the efficiencies of the components and the greater the power generation will be. The ambient temperature, however, plays a minor role in affecting power generation for the solar power plant.

It is concluded that the mathematical model is basically valid for the solar chimney thermal power generating system, and the simulation with the model can be used conveniently to predict the performance of the system, instead of using cumbersome and taxing experimental measurements.

Nomenclature

| | | | |
|------------------|---|----------------------|---|
| A_C | – cross area of chimney, [m ²] | Δp_{tot} | – the pressure difference, [kPa] |
| C_p | – specific heat capacity, [Jkg ⁻¹ K ⁻¹] | R | – radius, [m] |
| D | – chimney diameter, [m] | Ra | – Rayleigh number $Ra = Gr_H Pr = g\beta/\nu\alpha(T_s - T_\infty)H^3$, [-] |
| $E_{e,an}$ | – annual electric energy, [Wh per year] | R_t | – relative air pressure drop |
| f | – wall friction factor, [-] | r_b | – maintenance and repair costs 5.5% per year |
| G | – solar radiation, [Wm ⁻²] | r_t | – relative pressure drop in the turbine, [-] |
| G_b | – generation of turbulence kinetic energy due to buoyancy, [Jkg ⁻¹] | U | – total heat transfer coefficient from chimney air flow to atmospheric air, [Wm ⁻² K ⁻¹] |
| G_k | – generation of turbulence kinetic energy due to mean velocity gradients, [Jkg ⁻¹] | V | – velocity magnitude [ms ⁻¹] |
| H_{sc} | – height of the chimney, [m] | <i>Greek symbols</i> | |
| \dot{m} | – mass flow rate of hot air passing through the chimney, [kgs ⁻¹] | ε_{in} | – entrance loss coefficient |
| n | – amortization period, [year] | ε_{out} | – exit kinetic loss coefficient |
| P | – power, [kW] | η_{sp} | – overall efficiency of solar chimney, [%] |
| P_{out} | – electric power generated, [Wh per year] | η_{tg} | – efficiency of turbine generators, [%] |
| P_{tot} | – power contained in the flow, [kW] | <i>Subscripts</i> | |
| $P_{wt,max}$ | – maximum turbine power, [kW] | coll | – collector |
| p | – pressure, [Pa] | tg | – turbine generator |
| Δp | – pressure difference, [kPa] | | |
| Δp_f | – friction loss in the chimney, [kPa] | | |
| Δp_{in} | – entrance loss, [kPa] | | |
| Δp_{out} | – exit kinetic energy loss, [kPa] | | |

References

- [1] ***, <http://www.greenenergy-jo.com/Spaper/54.pdf>
- [2] Ming, T. Z., Liu, W., Pan, Y., Numerical Analysis of the Solar Chimney Power Plant with Energy Storage Layer, *Proceedings, ISES World Congress 2007, Vol. I-V (2009)*, 5, pp. 1800-1805
- [3] Nizetic, S., Ninic, N., Klarin, B., Analysis and Feasibility of Implementing Solar Chimney Power Plants in the Mediterranean Region, *33 (2008)*, 11, pp. 1680-1690

- [4] Zhou, X., Solar Potential for the Solar Photovoltaic Roof Integration System in China Explored by the Geographic Information System, *International Journal of Global Energy Issues*, 31 (2009), 1, pp. 50-60
- [5] ***, <http://www.greenenergy-jo.com/Spaper/48.pdf>
- [6] Ghazal, M., Jordan Turns to Renewable Energy to Power its Future
http://www.alshorfa.com/cocoon/meii/xhtml/en_GB/features/meii/features/main/2010/05/10/feature-02
- [7] Malek, K., Identification of National Energy Policies and Energy Access in Jordan, 2005
<http://webfea-lb.fe.aub.edu.lb/fea/research/erg/web/Policy%20Paper%20Jordan.pdf>
- [8] ***, Nur Solar Systems, Why Solar Energy, <http://www.nursolarsys.com/whysolar.html>
- [9] Al-Salaymeh, A., Modelling of Global Daily Solar Radiation on Horizontal Surfaces for Amman City, *Emirates Journal for Engineering Research*, 11 (2006), 1, pp. 49-56, 920060
- [10] ***, <http://www.undp Jordan.org/LinkClick.aspx?fileticket=ieOv%2btI2mqQ%3d&tabid=36&mid=373>
- [11] Ketlogetswe, C., *et al.*, Solar Chimney Power Generation Project, The Case for Botswana, *Renewable and Sustainable Energy Reviews*, 12 (2008), 7, pp. 2005-2012
- [12] Dai, Y., Case Study of Solar Chimney Power Plants in Northwestern regions of China, *Renewable Energy*, 28 (2003), 8, pp. 1295-1304
- [13] ***, <http://www.2b.abc.net.au/science/k2/stn/newposts/4525/topic4525447.shtm>
- [14] Quaschnig, V., Technology Fundamentals – Solar Thermal Power Plants, *Renewable Energy World*, 6 (2003), 6, pp. 109-113
- [15] Ming, T., M., *et al.*, Numerical Simulation of the Solar Chimney Power Plant Systems Coupled with Turbine, *Renewable Energy*, 33 (2008), 5, pp. 897-905
- [16] Huang, H., *et al.*, Simulation Calculation on Solar Chimney Power Plant System, *Challenges of Power Engineering and Environment*, 1 (2007), 14, pp. 1158-1161
- [17] Petela, R., Thermodynamic Study of a Simplified Model of the Solar Chimney Power Plant, *Solar Energy*, ASME, *J. Heat Transfer*, 93 (2009), 1, pp. 94-107
- [18] von Backström, T. W., Fluri, T. P., Maximum Fluid Power Condition in Solar Chimney Power Plants, An Analytical Approach, *Solar Energy*, 80 (2006), 11, pp. 1417-1423
- [19] Ming, T. Z., Numerical Analysis of Flow and Heat Transfer Characteristics in Solar Chimney Power Plants with Energy Storage Layer, *Energy Conversion and Management*, 49 (2008), 10, pp. 2872-2879
- [20] Zhou, X., Simulation of a Pilot Solar Chimney Thermal Power Generating Equipment, *Renewable Energy*, 32 (2007), 10, pp. 1637-1644
- [21] ***, http://css.engineering.uiowa.edu/~fluids/lecture_notes/Chapter_6/Chapter_6.pdf
- [22] Nizetic, S., A Simplified Analytical Approach for Evaluation of the Optimal Ratio of Pressure Drop Across the Turbine in Solar Chimney Power Plants, *Applied Energy*, 87 (2010), 2, pp. 587-591
- [23] Fung-Bao Liu, An Experimental and Numerical Investigation of Fluid Flow in a Cross-Corrugated Channel, *Heat and Mass Transfer*, 46 (2010), 5, pp. 585-593,
- [24] Ming T. Z., *et al.*, Numerical Simulation of the Solar Chimney Power Plant Systems Coupled with Turbine, *Renewable Energy*, 33 (2008), 5, pp. 897-905
- [25] Zhou, X., Night Operation of Solar Chimney Power System Using Solar Ponds for Heat Storage, *International Journal of Global Energy*, 31 (2009), 2, pp. 193-207
- [26] Zhou, X., Novel Concept for Producing Energy Integrating a Solar Collector with a Man Made Mountain Hollow, *Energy Conversion and Management*, 50 (2009), 3, pp. 847-854
- [27] Zhou, X., Comparison of Classical Solar Chimney Power System and Combined Solar Chimney System for Power Generation and Seawater Desalination, *Desalination*, 250 (2010), 1, pp. 249-256
- [28] Zhou, X., Performance of Solar Chimney Power Plant in Qinghai-Tibet Plateau, *Renewable and Sustainable Energy Reviews*, 14 (2010), 8, pp. 2249-2255
- [29] http://en.wikipedia.org/wiki/Solar_updraft_tower
- [30] dos S. Bernardes, M. A., Thermal and Technical Analyses of Solar Chimneys, *Solar Energy*, 75 (2003), 6, pp. 511-524
- [31] Zhou, X., *et al.*, Analysis of Chimney Height for Solar Chimney Power Plant, *Applied Thermal Engineering*, 29 (2009), 1, pp. 178-185
- [32] Koonsrisuk, A., Chitsomboon, T., Partial Similarity in Solar Tower Modeling, 20th Conference of Mechanical Engineering Network of Thailand, Nakhon Ratchasima, Thailand, 2006
- [32a] Koonsrisuk, A., Chitsomboon, T., Dynamic Similarity in Solar Chimney Modeling, *Solar Energy*, 81 (2007), 12, pp. 1439-1446
- [33] Fluri, T. P., Turbine Layout for and Optimization of Solar Chimney Power Conversion Units, Ph. D. thesis, University of Stellenbosch, Stellenbosch, South Africa
- [34] ***, http://www.sbp.de/de/html/projects/solar/aufwind/pages_auf/enprocos.htm

- [35] ***, <http://europe.theoil drum.com/story/2005/9/20/233641/494>
- [36] Haaf, W., *et al.*, Solar Chimneys, *Int J Sol Energy*, 2 (1983), 2, pp. 3-20
- [37] Mava, B., Weinrebe, G., Thermal and Technical Analyzes of Solar Chimneys, *Sol Energy*, 75 (2003), 6, pp. 511-524
- [38] Pasthan, H., Kornadt, O., Gurlebeck, K., Numerical and Analytical Calculations of the Temperature and Flow Field in the Upwind Power Plant, *Int J Energy Res*, 28 (2004), 6, pp. 495-510
- [39] Schlaich, J., *et al.*, Design of Commercial Solar Updraft Tower Systems-Utilization of Solar Induced Convective Flows for Power Generation, *ASME J Sol Energy Eng.*, 127 (2005), 1, pp. 117-124
- [40] Ming, T. Z., *et al.*, Thermodynamic Analysis of Solar Chimney Power Plant System, *J Huazhong Univ Sci Technol*, 33 (2005), 8, pp. 1-4
- [41] Liu, W., *et al.*, Simulation of Characteristic of Heat Transfer and Flow for MW-Graded Solar Chimney Power Plant System, *J Huazhong Univ Sci Technol*, 33 (2005), 8, pp. 5-7
- [42] Bilgen, E., Rheault, J., Solar Chimney Power Plants for High Latitudes, *Solar Energy*, 79 (2006), 5, pp. 449-458
- [43] Pretorius, J. P., Kröger, D. G., Critical Evaluation of Solar Chimney Power Plant Performance, *Solar Energy*, 80 (2006), 5, pp. 535-544
- [44] Ming, T. Z., Liu, W., Xu, G. L., Study of the Solar Chimney Power Plant Systems, *J Eng Thermodynam*, 27 (2006), 3, pp. 505-507
- [45] Ming, T. Z., Liu, W., Xu, G. L., Analytical and Numerical Investigation of the Solar Chimney Power Plant Systems, *Int J Energy Res*, 30 (2006), 11, pp. 861-873
- [46] Zhou, X., *et al.*, Simulation of a Pilot Solar Chimney Thermal Power Generating Equipment, *Renew Energy*, 32 (2007), 10, pp. 1637-1644

Appendix

Main dimensions and operating parameters calculated for two pilot solar chimneys under two different conditions

Physical properties, main dimensions, and operating parameters of the pilot solar chimney in Mutah University

| | | |
|--|--|---|
| $R_{\text{coll}} = 3.4 \text{ m}$ | The cross-section area of the chimney = 0.2642 m^2 | $R_{\text{c in}} = 0.285 \text{ m}$ |
| $H = 4 \text{ m}$ | | $R_{\text{c out}} = 0.29 \text{ m}$ |
| Main collector roof high = 1 m | The area of the solar collector $A_{\text{coll}} = 36 \text{ m}^2$ | $h_{\text{in}} = 7.5 \text{ W/m}^2\text{C}$ |
| $V_{\text{in}} = 2 \text{ m/s}$ | $V_{\text{out}} = 0.5 \text{ m/s}$ | $h_{\text{out}} = 15 \text{ W/m}^2\text{C}$ |
| $\rho_{\text{out}} = 1.0 \text{ kg/m}^3$ | $\rho_{\text{in}} = 1.0 \text{ kg/m}^3$ | $k_{\text{steel}} = 59 \text{ W/m}^2\text{C}$ |
| $\gamma_{\infty} = 0.0065 \text{ K/m}$ | $G = 517 \text{ W/m}^2$ | $L_{\text{chimney}} = 4 \text{ m}$ |
| $\eta_{\text{coll}} = 0.6$ | $C_p = 1.0090 \text{ kJ/kgC}$ | $A_{\text{in}} = 7.16283 \text{ m}^2$ |
| $T_{\text{in}} = 305 \text{ K}$ | $T_{\text{out}} = 300 \text{ K}$ | $A_{\text{out}} = 7.2885 \text{ m}^2$ |

$$\dot{m} = \rho_{\text{in}} V_{\text{in}} A_c = 0.5808 \text{ kg/s}$$

$$\Delta p = 0.00353gH \left[\frac{\pi G \eta_{\text{coll}} R_{\text{coll}}^2}{c_p m} - \frac{g}{2c_p} H + \frac{1}{2} \gamma_{\infty} H \right] = 7.46545 \text{ kPa}$$

$$U_{\text{out}} = \frac{1}{\frac{A_o}{A_i} \frac{1}{h_i} + \frac{A_o \ln \frac{r_o}{r_i}}{2\pi k l} + \frac{1}{h_o}} = 0.1552 \text{ W/m}^2\text{C}$$

$$H_{\text{max.}} = \frac{c_p m}{U \pi D} \ln \left[\frac{\pi^2 U D G \eta_{\text{coll}} R_{\text{coll}}^2}{c_p m^2 (g - \gamma_{\infty} c_p)} + 1 \right] = 17.48523 \text{ m}$$

Physical properties, main dimensions, and operating parameters of the pilot solar chimney in Manzanares

| | | |
|--|---|---|
| $R_{\text{coll}} = 122 \text{ m}$ | Main roof high = 1.85 m | $\eta_{\text{coll}} = 0.6$ |
| $\rho_{\text{in}} = 1.00 \text{ kg/m}^3$ | $\rho_{\text{out}} = 1.177 \text{ kg/m}^3$ | $C_p = 1.0090 \text{ kJ/kgC}$ |
| $V_{\text{in}} = 7 \text{ m/s}$ | $V_{\text{out}} = 4 \text{ m/s}$ | $G = 1040 \text{ W/m}^2$ |
| $T_{\text{out}} = 300 \text{ K}$ | $T_{\text{in}} = 350 \text{ K}$ | $\gamma_{\infty} = 0.0065 \text{ K/m}$ |
| $A_{\text{coll}} = 46.76 \cdot 10^3 \text{ m}^2$ | $U_{\text{out}} = 0.07 \text{ W/m}^2\text{C}$ | The area of the chimney = 78.54 m^2 |
| $H = 200 \text{ m}$ | | |

$$\dot{m} = \rho_{\text{in}} V_{\text{in}} A_c = 549.78 \text{ kg/s}$$

$$\Delta p = 0.00353gH \left[\frac{\pi G \eta_{\text{coll}} R_{\text{coll}}^2}{C_p \dot{m}} - \frac{g}{2C_p} H + \frac{1}{2} \gamma_{\infty} H \right] = 12.153221 \text{ kPa}$$

The power output is:

$$\Delta p = \Delta p_t + \Delta p_f + \Delta p_{\text{in}} + \Delta p_{\text{out}}$$

where

$$\Delta p_{\text{out}} = \varepsilon_{\text{out}} \frac{1}{2} \rho_{\text{out}} V_{\text{out}}^2 = 9.962128 \text{ pu}$$

$$\Delta p_{\text{in}} = \varepsilon_{\text{in}} \frac{1}{2} \rho_{\text{in}} V_{\text{in}}^2 = 1.372 \text{ Pa}$$

$$\Delta p_{\text{f}} = f \frac{H}{D} \frac{1}{2} \rho V^2 = 4.12972 \text{ Pa}$$

So,

$$\Delta p_{\text{t}} = 12.14889 \text{ kPa}$$

$$P_{\text{out}} = \eta_{\text{tg}} \Delta p_{\text{t}} V A_{\text{C}} = 37.852 \text{ kW}$$

and to calculate the efficiency of the system:

$$\eta = \frac{P_{\text{out}}}{\pi R_{\text{coll}}^2 G} = 0.077$$

Substituting in equation for $H_{\text{max.}}$:

$$H_{\text{max.}} = \frac{C_{\text{p}} \dot{m}}{U \pi D} \ln \left[\frac{\pi^2 U D G \eta_{\text{coll}} R_{\text{coll}}^2}{C_{\text{p}} \dot{m}^2 (g - \gamma_{\infty} C_{\text{p}})} + 1 \right] = 785.004 \text{ m}$$